

High-Mobility Air-Stable n-Type Semiconductors with Processing Versatility: Dicyanoperylene-3,4:9,10-bis(dicarboximides)**

Brooks A. Jones, Michael J. Ahrens, Myung-Han Yoon, Antonio Facchetti, Tobin J. Marks,* and Michael R. Wasielewski*

Traditionally, inorganic materials have been the active charge-transporting components in numerous electronic devices. While inorganic materials are ideal for many applications, the rapid development of molecular/polymeric semiconductors for organic field-effect transistors (OFETs) promises materials better suited to inexpensive, flexible, large-area applications, such as displays, RF-ID tags, smart cards, and sensors.^[1] To this end, recent advances in p-type organic semiconductors have fulfilled many of the requirements for use in diverse applications,^[1c-e,2] however, n-type materials, needed for complementary circuits, continue to present challenges, such as low mobilities, instability in air, poor solubility for efficient film-casting, and large barriers to electron injection.^[1b,2]

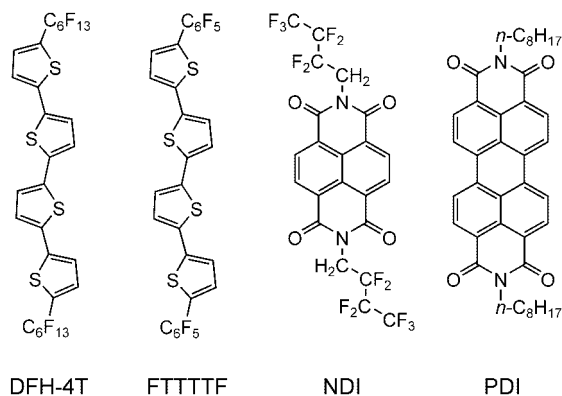
We have already demonstrated that high-mobility n-type organic semiconductors can be realized by functionalizing oligothiophene cores with electron-withdrawing perfluorinated groups (e.g. DFT-4T and FTTTTF).^[3] Furthermore, other research has demonstrated that electron-withdrawing imide substituents afford promising architectures for n-type naphthalene and perylene-based OFET materials (e.g., NDI and PDI).^[4] Thus, vapor-deposited and solution-cast films of *N*-fluorocarbon NDI derivatives exhibit air-stable n-type mobilities as high as $0.1 \text{ cm}^2 \text{ V}^{-1} \text{ s}^{-1}$, $I_{\text{on}}/I_{\text{off}} \approx 10^5$, and threshold voltages of approximately 20 V.^[4f-h] However, while *N*-alkyl NDI derivatives exhibit comparable or superior electrical performance, they fail to operate in air, possibly because of the less densely packed hydrocarbon tails.^[4f] While *N*-alkyl PDI films exhibit outstanding mobilities of approximately $0.6 \text{ cm}^2 \text{ V}^{-1} \text{ s}^{-1}$, OFET performance again degrades in air,

[*] B. A. Jones, M. J. Ahrens, M.-H. Yoon, Dr. A. Facchetti, Prof. T. J. Marks, Prof. M. R. Wasielewski
Department of Chemistry
Center for Nanofabrication and Molecular Self-Assembly
and the Materials Research Center
Northwestern University
2145 Sheridan Road, Evanston IL, 60208-3113 (USA)
Fax: (+1) 847-491-2290
E-mail: t-marks@northwestern.edu
wasielew@chem.northwestern.edu

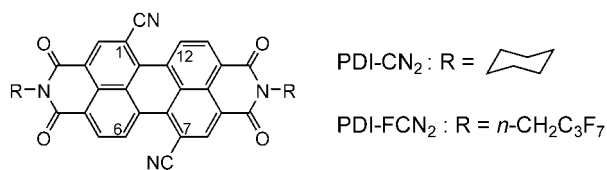
[**] We thank DARPA (MDA972-03-1-0023) and ONR (N00014-02-1-0909, N00014-02-1-0381) for support of this research, and the Northwestern Materials Research Center (NSF-MRSEC DMR-0076097) for characterization facilities. We also thank Charlotte Stern for single-crystal X-ray diffraction data collection and Matthew Russell for aid with SEM measurements.



Supporting information for this article is available on the WWW under <http://www.angewandte.org> or from the author.



devices exhibit very large threshold voltages of around 75 V, and these materials are not known to be solution processable.^[4d,i,k] In all instances, the focus of this prior work has been synthetic modification solely of the *N*-substituents. In other studies, microwave conductivity measurements of 1,6,7,12-substituted PDI derivatives demonstrated that modulation of π - π overlap by twisting of the normally flat core can drastically affect carrier mobility,^[4c] however, to date functionalization of the PDI core for OFET applications has gone unexplored. Herein we report two core-cyanated PDI derivatives, PDI-CN₂ and PDI-FCN₂, which exhibit the highest air-



stable n-type OFET carrier mobilities reported to date, in combination with low threshold voltages and substantial processing versatility.

The synthesis of PDI-CN₂ was reported elsewhere.^[5] This compound exhibits excellent air-stability and solubility in organic solvents, while reduced pressure thermogravimetric analysis (TGA) scans indicate slight (about 2%) decomposition during sublimation. The low-energy LUMO indicated by the first reduction potential, −0.07 V versus the saturated calomel electrode (SCE),^[5] suggests improved n-type charge-carrier stability over PDI (−0.43 V vs. SCE).^[6,7] Moreover, the results with PDI-CN₂-derived OFETs (see below) motivated the synthesis of a new PDI derivative, PDI-FCN₂, with additional electron-withdrawing substituents and greater volatility. The new compound was synthesized using modifications of published core cyanation^[5] and *N*-fluoroalkylation^[4f,j] procedures, and was characterized by NMR spectroscopy, mass spectrometry, optical absorption spectroscopy, photoluminescence, cyclic voltammetry, thermogravimetric analysis, and single-crystal X-ray diffraction. The electro-

chemical and optical data (Table 1) reveal further depression of the LUMO level of PDI-FCN₂ compared to PDI and PDI-CN₂, while TGA indicates quantitative sublimation.

For both cyanated PDI materials, a 1:1 mixture of isomers (cyanated at the 1,7 or 1,6 positions) is indicated by NMR spectroscopy, however this characteristic is found to be inconsequential for spectroscopic, electronic structural, and solid-state charge-transport properties (verified by measurements on the pure 1,7 isomer). Single crystals of PDI-FCN₂ were grown by sublimation, and the crystal structure (Figure 1) reveals a slightly twisted polycyclic core (torsion angle of about 5°) with slip-stacked face-to-face molecular packing and a minimum interplanar spacing of 3.40 Å.^[8] This

Table 1: Electronic and OFET characteristics of perylene diimide derivatives.

Compound	λ_{abs} [nm] ^[a]	λ_{em} [nm] ^[a]	$E_{(1)}$ [V] ^[b]	$E_{(2)}$ [V] ^[b]	μ [cm ² V ^{−1} s ^{−1}]	$I_{\text{on}}/I_{\text{off}}$
PDI-CN ₂	530	547	−0.07	−0.40	0.10	10 ⁵
PDI-FCN ₂	530	545	+0.04	−0.31	0.64	10 ⁴

[a] measured in THF (10^{−5}/10^{−6} M). [b] Measured in a solution of 0.1 M tetrabutylammonium hexafluorophosphate (TBA PF₆) in THF versus SCE.

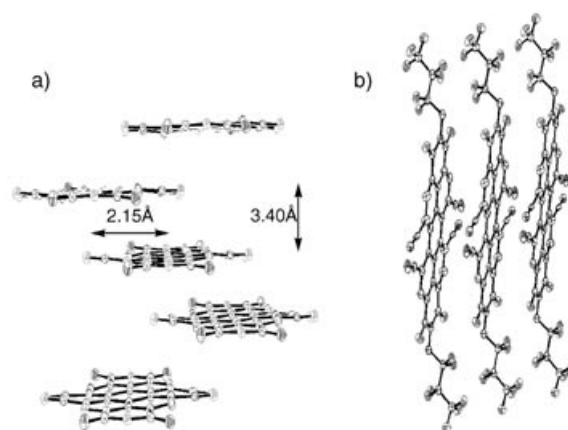


Figure 1. Crystal Structure of PDI-FCN₂. a) viewed along the unit cell diagonal, showing stacking relationships; fluoropropyl groups deleted for clarity. b) Viewed along the *ab* face diagonal, showing the segregation of arene and fluoroalkyl groups. Note the statistical disorder of the cyano substituents.^[10]

motif allows considerable intermolecular π - π overlap, which results in good charge-transport properties (see below). The positions of the disordered cyano substituents suggests that this structural feature does not greatly affect packing.

Top-contact configuration OFETs were fabricated with vapor-deposited PDI films (10^{−6} Torr, 0.2 Å s^{−1} growth), and mobilities determined in the saturation regime by standard procedures.^[3] The microstructures and mobilities of the vapor-deposited films are found to be sensitive to substrate temperature during growth (see Supporting Information^[9]). Owing to the remarkable air-stability of these materials, all data presented herein were acquired under ambient atmosphere. PDI-CN₂-based OFETs display mobilities as high as 0.10 cm²V^{−1}s^{−1}, threshold voltages of approximately 15 V,

and $I_{\text{on}}/I_{\text{off}}(+100\text{ V}/0\text{ V}) \approx 10^5$, while PDI-FCN₂ devices exhibit mobilities as high as $0.64\text{ cm}^2\text{ V}^{-1}\text{ s}^{-1}$, threshold voltages between -20 V and -30 V , and $I_{\text{on}}/I_{\text{off}}(+100\text{ V}/-60\text{ V})$ as high as 10^4 . Figure 2 shows current–voltage (I – V) characteristics between source and drain electrodes recorded at different gate biases (V_G) for OFETs of PDI-CN₂ and PDI-FCN₂ operating in ambient atmosphere. Given the similarities in first reduction potentials for PDI-CN₂ and PDI-FCN₂, the striking difference in threshold voltages is presumably due to variations in trap densities in the two materials. Devices stored and tested under ambient conditions exhibit negligible degradation in mobility, threshold voltage, or $I_{\text{on}}/I_{\text{off}}$ over six months.

The microstructure of the vapor-deposited thin films was analyzed by X-ray diffraction (XRD), atomic force microscopy (AFM), and scanning electron microscopy (SEM), with XRD revealing d -spacings in highest-mobility devices of 17.9 Å for PDI-CN₂ and 20.3 Å for PDI-FCN₂. From a geometry-optimized, computed molecular length of 22.0 Å for PDI-CN₂^[11] and a crystallographically determined length of 22.8 Å for PDI-FCN₂, tilt angles relative to the substrate normal of 55° for PDI-CN₂ and 62° for PDI-FCN₂ are estimated. These results suggest favorable molecular orientations for source-to-drain electrode charge transport.

AFM and SEM analysis of film morphology confirms polycrystalline topologies with ribbon-like grains (ca. 400 – 800 nm long, and ca. 100 nm wide).^[9] Such large-grained polycrystalline features should promote charge-carrier mobility through efficient π – π intermolecular overlap and minimization of trap sites.^[1c,12]

To investigate material versatility for various applications, preliminary studies on bottom-contact OFETs and solution-cast films were performed. Bottom-contact devices are found to display air-stable mobilities from 10^{-3} – $10^{-4}\text{ cm}^2\text{ V}^{-1}\text{ s}^{-1}$. PDI-FCN₂ transistors, like many fluorinated organic semiconductors, require alkane thiol treatment of gold electrodes to better match surface energies at the metal/organic interface.^[4g] PDI-CN₂ devices function without the aid of thiolated electrodes, retaining the ability of PDI to function on unmodified substrates.^[4i] Top-contact devices fabricated from drip-cast films are also air-stable and exhibit mobilities of 10^{-3} – $10^{-5}\text{ cm}^2\text{ V}^{-1}\text{ s}^{-1}$. In contrast, solution casting of high-

quality films of PDI derivatives not having core functionalization is difficult owing to low solubility in common solvents. While the performance of the vapor-deposited top-contact devices is currently superior to the bottom-contact and solution-cast devices, efforts are being made to optimize device performance in these latter configurations.

One of the unique characteristics of the new PDI systems is the presence of significant charge-carrier densities at $V_G = 0\text{ V}$. Thus, the OFET threshold voltages for these materials are at $V_G = -20\text{ V}$ to -30 V , with the absence of charge carriers then defining the “off” state at -60 V , and classifying these devices as “always on” transistors.^[13] This characteristic is documented for very electron-deficient materials, and often attributed to unintentional doping.^[14] In some cases, the presence of charge carriers below $V_G = 0\text{ V}$ can be reversed by exposure to an oxidant, and for our devices, I₂ vapor increases the threshold voltage to $> -5\text{ V}$ and decreases the I_{SD} at $V_G = 0\text{ V}$ by up to an order of magnitude. Further studies of the nature and origin of the charge carriers are currently underway.

It is thought that ambient stability in n-type organic semiconductors benefits from electron-withdrawing fluorinated substituents, which electronically stabilize the charge carriers as well as promote close packing through fluorocarbon self-segregation. Judging from the present redox potentials, the charge carriers are not expected to be stable with respect to gaseous O₂;^[15] however, the close-packed fluorine functionalities may help provide a kinetic barrier to oxidation.^[1c] The strategic cyanation of PDI produces air-stable *N*-fluoroalkyl and *N*-alkyl materials, the air stability presumably reflecting carrier stabilization in the very low-lying LUMOs.

In summary, we report a promising new class of solution processable, cyano-polycyclic n-type organic semiconductors with high carrier mobility and air-stable OFET operation. Notable properties of this family reflect a combination of functionality at the core and imide positions. The cyano functionalities provide solubility for solution processing and stability of n-type charge carriers by lowering the LUMO to resist ambient oxidation. The electron-withdrawing *N*-functionalities further aid charge carrier stability by further lowering the LUMO energies, but may also induce close molecular packing for increased intermolecular π overlap and

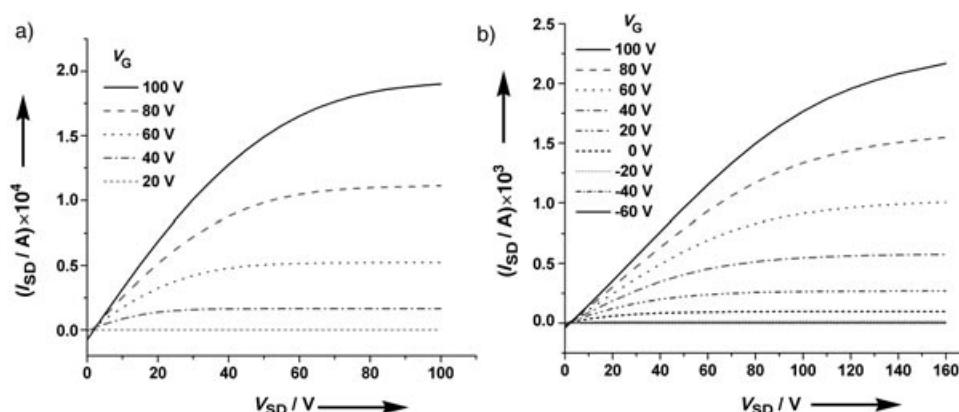


Figure 2. a) I – V characteristics of PDI-CN₂ exhibiting a mobility of $0.10\text{ cm}^2\text{ V}^{-1}\text{ s}^{-1}$ in ambient atmosphere b) I – V characteristics of a PDI-FCN₂ FET exhibiting a mobility of $0.64\text{ cm}^2\text{ V}^{-1}\text{ s}^{-1}$ in ambient atmosphere. V_{SD} = Voltage between source and drain, I_{SD} = current between source and drain, V_G = gate voltage.

more efficient charge transport. With the rich chemistry for PDI functionalization available, these derivatives should prove informative for elucidating structure–function relationships in organic n-type electronics.

Received: July 15, 2004

Keywords: conducting materials · electron transport · perylenes · semiconductors

- [1] a) B. Crone, A. Dodabalapur, A. Gelperin, L. Torsi, H. E. Katz, A. J. Lovinger, Z. Bao, *Appl. Phys. Lett.* **2001**, 78, 2229; b) C. D. Dimitrakopoulos, D. J. Maseo, *IBM J. Res. Dev.* **2001**, 45; c) C. D. Dimitrakopoulos, P. R. L. Malenfant, *Adv. Mater.* **2002**, 14, 99; d) A. Kraft, *ChemPhysChem* **2001**, 2, 163; e) F. Würthner, *Angew. Chem.* **2001**, 113, 1069; *Angew. Chem. Int. Ed.* **2001**, 40, 1037.
- [2] Z. Bao, *Adv. Mater.* **2000**, 12, 227.
- [3] a) A. Facchetti, Y. Deng, A. Wang, Y. Koide, H. Sirringhaus, T. J. Marks, R. H. Friend, *Angew. Chem.* **2000**, 112, 4721; *Angew. Chem. Int. Ed.* **2000**, 39, 4547; b) A. Facchetti, M. Mushrush, H. E. Katz, T. J. Marks, *Adv. Mater.* **2003**, 15, 33; c) A. Facchetti, M.-H. Yoon, C. L. Stern, H. E. Katz, T. J. Marks, *Angew. Chem.* **2003**, 115, 4030; *Angew. Chem. Int. Ed.* **2003**, 42, 3900.
- [4] a) M. A. Angadi, D. Gosztola, M. R. Wasielewski, *J. Appl. Phys.* **1998**, 83, 6187; b) M. A. Angadi, D. Gosztola, M. R. Wasielewski, *Mater. Sci. Eng. B* **1999**, 191; c) Z. Chen, M. G. Debijs, T. Debaerdemaeker, P. Osswald, F. Würthner, *ChemPhysChem* **2004**, 5, 137; d) R. J. Chesterfield, J. C. McKeen, C. R. Newman, C. D. Frisbie, P. C. Ewbank, K. R. Mann, L. R. Miller, *J. Appl. Phys.* **2004**, 95, 6396; e) G. Horowitz, F. Kouki, P. Spearman, D. Fichou, C. Nogués, X. Pan, F. Garnier, *Adv. Mater.* **1996**, 8, 242; f) H. E. Katz, A. J. Lovinger, J. Johnson, C. Kloc, T. Siegrist, W. Li, Y.-Y. Lin, A. Dodabalapur, *Nature* **2000**, 404, 478; g) H. E. Katz, J. Johnson, A. J. Lovinger, W. Li, *J. Am. Chem. Soc.* **2000**, 122, 7787; h) H. E. Katz, T. Siegrist, J. H. Schön, C. Kloc, B. Batlogg, A. J. Lovinger, J. Johnson, *ChemPhysChem* **2001**, 2, 167; i) P. R. L. Malenfant, C. D. Dimitrakopoulos, J. D. Gelorme, L. L. Kosbar, T. O. Graham, A. Curioni, W. Andreoni, *Appl. Phys. Lett.* **2002**, 80, 2517; j) M.-M. Shi, H.-Z. Chen, J.-Z. Sun, J. Ye, M. Wang, *Chem. Commun.* **2003**, 14, 1710; k) C. W. Struijk, A. B. Sieval, J. E. J. Dakhorst, M. Van Dijk, P. Kimkes, R. B. M. Koehorst, H. Donker, T. J. Schaafsma, S. J. Picken, A. M. van de Craats, J. M. Warman, H. Zuilhof, E. J. R. Sudholter, *J. Am. Chem. Soc.* **2000**, 122, 11057.
- [5] M. J. Ahrens, M. J. Fuller, M. R. Wasielewski, *Chem. Mater.* **2003**, 15, 2684.
- [6] a) D. Gosztola, M. P. Niemczyk, W. Svec, A. S. Lukas, M. R. Wasielewski, *J. Phys. Chem. A* **2000**, 104, 6545; b) For a compilation of redox potentials, see: F. Würthner, *Chem. Commun.* **2004**, 1564.
- [7] a) A. Facchetti, M.-H. Yoon, C. L. Stern, G. Hutchison, M. A. Ratner, T. J. Marks, *J. Am. Chem. Soc.* **2004**, 126, 13480; b) A. Facchetti, M. Mushrush, M.-H. Yoon, G. R. Hutchison, M. A. Ratner, T. J. Marks, *J. Am. Chem. Soc.* **2004**, 126, ASAP.
- [8] Single crystals were grown by slow vacuum sublimation. Crystal size: 0.345 mm × 0.106 mm × 0.022 mm. Triclinic, $P\bar{1}$, $Z = 1$. Cell dimensions: $a = 5.2320(14)$, $b = 7.638(2)$, $c = 18.819(5)$ Å; $\alpha = 92.512(5)^\circ$, $\beta = 95.247(5)^\circ$, $\gamma = 104.730(4)^\circ$, $V = 722.5(3)$ Å³, $2\theta_{\max} = 57.54^\circ$, $\rho_{\text{calcd}} = 1.849$ g cm⁻³. Of 6655 reflections, 3370 were independent ($R_{\text{int}} = 0.0967$), 272 parameters, $R1 = 0.0540$ (for reflections with $I > 2\sigma(I)$), $wR2 = 0.1258$ (for all reflections). All diffraction measurements were made on a Bruker SMART CCD diffractometer with graphite monochromated MoK α radiation. Data were collected at 153(2) K and the structure

solved by direct methods using SHELXTL. All non-hydrogen atoms were refined anisotropically. Hydrogen atoms were included in idealized positions and not refined. Intensities were corrected for absorption. CCDC-247498 contains the supplementary crystallographic data for this paper. These data can be obtained free of charge via www.ccdc.cam.ac.uk/conts/retrieving.html (or from the Cambridge Crystallographic Data Centre, 12 Union Road, Cambridge CB21EZ, UK; fax: (+44) 1223-336-033; or deposit@ccdc.cam.ac.uk).

- [9] See Supporting Information which includes: Experimental details, TGA plots, thin film XRD data, SEM, and AFM micrographs, redox properties of PDI derivatives, and details of device fabrication/measurement.
- [10] M. N. Burnett and C. K. Johnson, ORTEP-III: Oak Ridge Thermal Ellipsoid Plot Program for Crystal Structure Illustrations, Oak Ridge National Laboratory Report ORNL-6895, 1996.
- [11] Hyperchem (TM) 5.02, Hypercube, Inc., 1115 NW 4th Street, Gainesville, FL 32601, USA.
- [12] a) G. Horowitz, *Adv. Mater.* **1998**, 10, 365; b) H. E. Katz, Z. Bao, *J. Phys. Chem. B* **2000**, 104, 671.
- [13] S. M. Sze, *Semiconductor Devices*, Wiley, New York, **1985**.
- [14] a) R. C. Haddon, A. S. Perel, R. C. Morris, T. T. M. Palstra, A. F. Hebard, R. M. Fleming, *Appl. Phys. Lett.* **1995**, 67, 121; b) T. M. Pappenfus, R. J. Chesterfield, C. D. Frisbie, K. R. Mann, J. Casado, J. D. Raff, L. L. Miller, *J. Am. Chem. Soc.* **2002**, 124, 4184; c) J. G. Laquindanum, H. E. Katz, A. Dodabalapur, A. J. Lovinger, *J. Am. Chem. Soc.* **1996**, 118, 11331.
- [15] D. M. de Leeuw, M. M. J. Simenon, A. R. Brown, R. E. F. Einerhand, *Synth. Met.* **1997**, 87, 53.